SLAC-PUB-3023
November 1982
(M)

MORE ON DESIGN OF LINEAR SOLAR ENERGY COLLECTORS HAVING SPHERICAL REFLECTORS

F. F. Hall
Stanford Linear Accelerator Center
Stanford University
Stanford, California 94305, U.S.A.

ABSTRACT

A number of design refinements for the basic system were discussed at MICAES IV. Net effect was increased operating temperature and concentration factors at the expense of solar energy collection efficiency. This paper discusses revisions needed to effect a more balanced overall system performance. Some items result in subsystem improvements. Notably the collection probe diameter is increased so as to obviate need for auxiliary support cables. The larger probe diameter also permits the adoption of a simpler and lighter weight probe construction system. The overall effect of lower concentration factors is reviewed. For thermal systems the heat collected per unit of collection area will be increased at lower collection temperatures. Happily, it is possible to use lower temperature and/or pressure steam turbine-generator sets having reasonably good engine efficiencies. For photo-electric applications the power flux can be much less, which is beneficial. Each of the revisions is described in some detail. An updated set of design parameters is appended.

1. PROBLEMS

Last year the weightless balloon reflector system was further described [1]. Concurrently with the preparation of that paper a review was made of the concepts which developed a number of problem areas [2]. These had to do with the following:

The assumed concentration factors were improbably high. The rationale is that the sun's rays spread from a 1,300,000 Km wide source located 150,000,000 Km away and arrive in a spread formation. This, coupled with the imperfections of the mirrored surface of a balloon, results in further spread. The resultant spread requires a linear collector which has a larger diameter and a concentration factor of 75 which will limit the temperature of collection of a thermal system.

Ideas for reducing wastage of balloon skin material, as shown then, foundered on the harsh realities of the two-way curvature of a spherical surface. Conventional approaches result in 20-50% wastage and earlier improvements considered require so many film strip cross snips as to make assembly very complicated.

The passage of sun's rays through the outer portions of the clear balloon hemisphere is at bad angles. The more extreme outer rays have to be double

* Work supported by the Department of Energy, contract DE-AC03-76SF00515.

Presented at the 5th Miami International Conference on Alternate Energy.
Miami Beach, Flordia, December 13 - 15, 1982.

bounced to reach the linear collector. Many single-bounced rays arrive near the collector outer tip also at bad angles. All of this results in the possibility that, as shown, only 72% of the reflective surface may be of assured usefulness.

2. SOLUTIONS

Studying the total ramifications of these postulated shortcomings required considerable effort, as one cannot veto the premises of basic engineering or physics.

One possibility was to have the balloon halves be opposed cones. Forgetting structural difficulties for a moment, this would require sacrifice of size, shape and weightlessness which, per se, are expendable. All sun's rays would cross the clear film at the same angle. The reflected rays would impinge on collectors (absorbers) at very good angles. Two cones within a sphere have less surface material. This sounds great, but the collector must be two to four times longer and the concentration factor drops to 45 plus or minus 5.

Giving up on opposed cones brings us back to spheres, which is a natural shape for balloons. In thinking about how to make a sphere at minimal skin wastage, I studied a toy balloon. It had six large sextant panels and two polar circle panels. Since main panels can be made using many gores or subpanels, the wastage problem is all but eliminated. The subpanels could be concentric, as previously shown, but this compounds the third problem. Extreme sun's rays have progressively more difficulty seeing in past the circular seam tapes. This is solved by placing the subpanels at right angles to the balloon equator. Further reflection indicated that the use of eight main panels, each consisting of an equilateral polar triangle having 90° corner angles, allows an easy construction. The general arrangement for a 32m diameter balloon is shown in Fig. 1.

Now the extreme sun's rays can see in unimpeded, except by increasing reflectance, all the way to the balloon equator. A penalty of 10% of available solar energy is assessed due to bad reflectance at the collection area perimeter. Fig. 2 shows the construction of the main panel layout for a 32m diameter balloon. Fig. 3 gives key dimensions for reflective and clear main panels (8 per balloon) and how gores can be cut to all but eliminate wastage, again for a 32m diameter balloon. Fig. 4 shows the appearance of the clear hemisphere as seen from the sun.

In considering the various inadequacies of thermal energy collection, it became clear that aluminized plastic film should not be used. There are two primary reasons. First, regenerative feed water heating steam cycles could not be used because hot primary coolant returns would heat balloon fill gas at balloon skin surface above plastic service temperatures close to the collector (absorber). Second, aluminized plastic reflectivity at 0.76 gives away too much [3]. Fortunately, mirrored, heavy high-purity aluminum foil at a reflectivity of 0.91 [3], backed by glass cloth reinforcement, can be used with seam tapes having high temperature-resistant sodium silicate adhesive which can be cured at room temperature. The use of cryogenically dried, oxygen-free nitrogen balloon fill gas will assure retention of the excellent reflectance of the aluminum sheets (and make large balloons weightless).

In considering collector design it is clear that earlier designs were forced in order to improve shape and increase concentration factors to achieve higher temperatures. While the higher temperatures are attainable, practical collection efficiencies are not. Conceding that very high collection temperatures can be achieved only by parabolic collectors allows a simplistic solution.

A helically wound tubing arrangement is shown in Fig. 5. The tubing toward the tip alternately presents good and bad angles to the incident sun's rays. The rays arriving at bad angles will reflect into the next coil turn at good angles and a cooled sun-end plate at collector tip will intercept worst angle reflections. A by-product benefit of larger diameter collectors is that these can be cantilevered to further simplify overall system construction by obviating the need for free end support cables.

Balloon collectors of solar energy could also be paraboloid, but this requires more skin material than for spherical collectors of the same diameter. Collection tolerances appear to exceed the capability of balloon makers and the support of an inverted cup collector is an interesting problem which I will look into when time permits. The possibility of helically winding strips of photo-voltaic cells around a linear collector is of obvious interest, but awaits the advance of technology to lower the collector cost to practical levels. Collectors discussed below are for thermal heat applications.

There are two general cases. One is low temperature collection at low pressure using water as the heat transfer medium. The other is high temperature collection using a medium which can be at high temperature and at low pressure such as liquid sodium-potassium eutectic alloy (NAK) which is liquid about 262^{O}K. The collector tubing coil is the same in either case with water coolant flow at 2m/s or NAK flowing at 16m/s. Coolant friction losses are low and similar for the two cases due to the much higher viscosity of water.

The NAK coolant flow rate has to be 7.5 times greater due to its poor heat capacity and larger temperature rise. Collector tubing would be seamless type 304 stainless steel. Heated coolant return tube is straight and runs down the centerline of the outer helically wound heat pick-up coil. Coils are terminated by two end plates. The mirror end plate furnishes an anchorage for the balloon skin and is attached to a mount which can be turned horizontally and tilted up and down to track the sun. Tubing assemblies will be brazed to be vacuumtight and add selective surface.

The concentration factor limit in turn limits the collection temperature to about 717^{O}K [3]. The 12,650 KW AIEEE/ASME preferred standard steam turbine unit had throttle steam at 714^{O}K and 40 atma pressure. It had 4-stage regenerative heating returning condensate to boilers at 449^{O}K and a heat rate of 3 Kwt/Kwe. Such a unit can be the low pressure turbine in a tandem arrangement.

Steam can be expanded from 700^{O}K, 136 atma to 526^{O}K, 42 atma in a high pressure turbine and then be reheated to 714^{O}K, 40 atma. The two turbines drive a single generator and the indicated dual heat steam electric heat rate is improved to 2.47 Kwt/Kwe. See Fig. 6.

To do this requires four heat exchangers. The feedwater heater (FWH) raises water temperature to 609^{O}K. The boiler (BLR) boils water at 609^{O}K. A superheater (SUP) raises steam temperature to 700^{O}K. A reheater (REH) raises steam temperature from 526^{O}K to 714^{O}K. Since heat is supplied from the liquid NAK, these heat exchangers can all be of the platefin type which are very lightweight and compact as compared to fuel burning plant equipment.

The foregoing cycle is based on a postulated maximum collection temperature of 717^{O}K at the sun-end tip of the collector tubing coil. Since collection efficiency improves as collection temperatures are dropped, a similar cycle having a maximum temperature of 659^{O}K was studied but, while collection efficiency improved 2%, the indicated thermal-electric efficiency was 6% lower and the cost of collectors per Kwe rose by 13% or more.

Attached is Table 1 containing data regarding the design parameters of the above-described solar energy collection system based on thermal heat collection for the reason noted above. I also hope to assemble a small working model (heat only, no electricity) during November, but make no promises.

REFERENCES

1. Hall, F.F. "Design Refinements for a Sun-Tracking Solar Energy Receiver having a Spherical Reflector," MICAES IV, Miami Beach (1981).

2. Brown, M. Report #007227 on Spherical Balloon Collectors to the OERI of the USDOC (1981).

3. Duffie, J.A., and Beckman, W.A. "Solar Energy Processes," pg. 105, or pg. 187, John Wiley and Sons (1974).

BASIC ARRANGEMENT FOR AN 804 m^2 SOLAR ENERGY COLLECTING BALLOON HAVING A DIAMETER OF 32 m

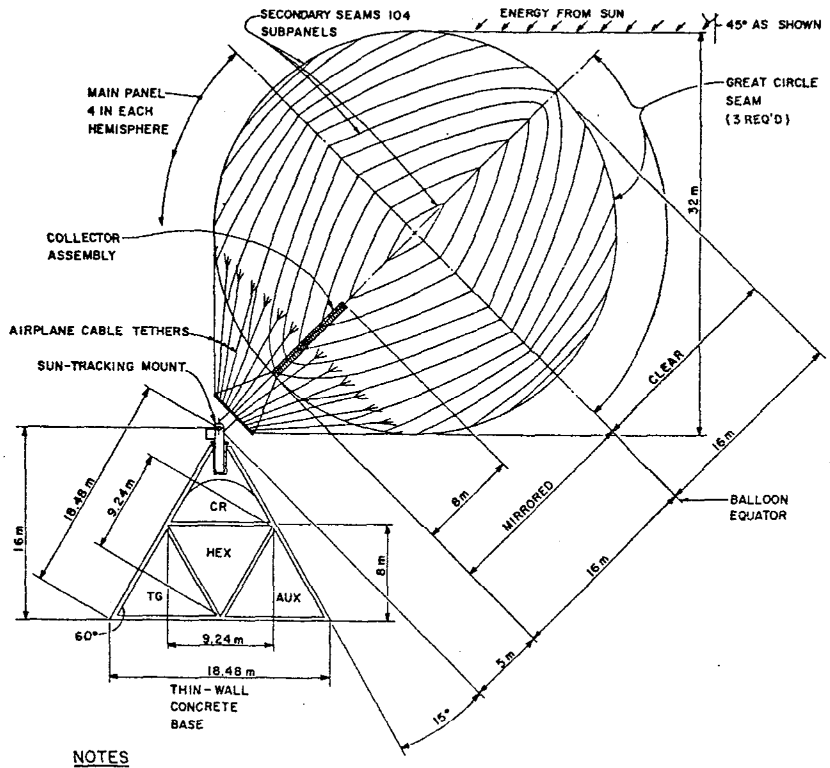

NOTES

1. CLEAR HEMISPHERE IS 0.0001m THICK POLYVINYL FLUORIDE (PVF) FILM REINFORCED BY POLYESTER MESH.
2. MIRRORED HEMISPHERE IS 0.0001m THICK ALUMINUM SHEET BACKED BY GLASS CLOTH.
3. BALLOON FILL GAS IS DRY NITROGEN AT 1.012 ATMA TO OFFSET NULL-POINT WIND PRESSURE AT 161 Km/Hr.

FIG. 1

MAIN PANEL LAYOUT FOR A 32 m DIAMETER SPHERE

NOTES

1. 8 MAIN PANELS REQ'D.
2. FOR SUBPANEL OR GORE ARRANGEMENT SEE FIG. 3.
3. THIS FIGURE SHOWS THE CONSTRUCTION OF A MAIN PANEL WHICH IS 1/8 Th OF THE SPHERE SURFACE.
4. THE MAIN PANEL IS AN EQUILATERAL POLAR TRIANGLE HAVING 90° CORNER ANGLES.

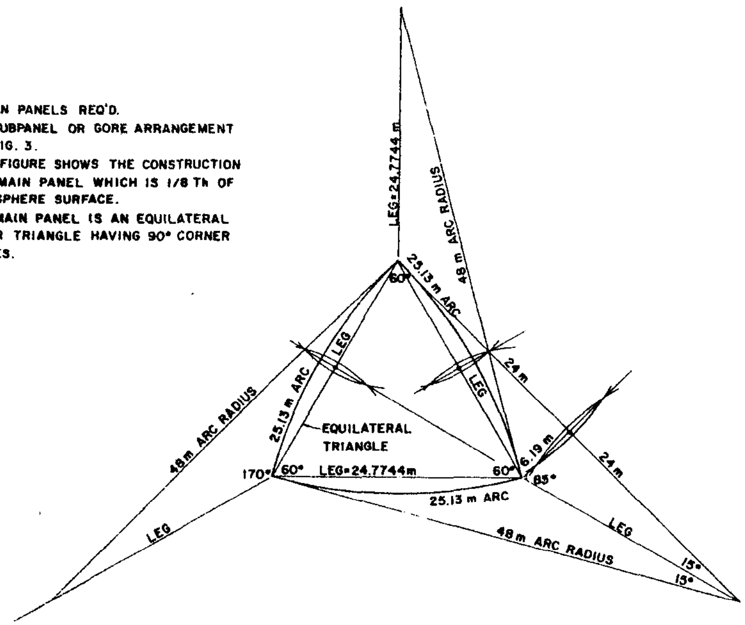

FIG. 2

MAIN SKIN PANELS FOR A 32 m DIAMETER BALLOON

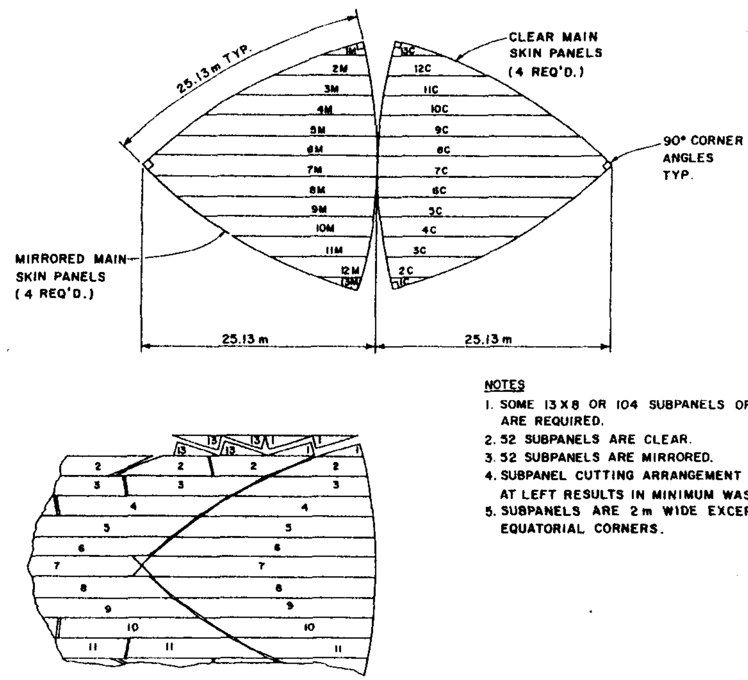

NOTES

1. SOME 13 X 8 OR 104 SUBPANELS OR GORES ARE REQUIRED.
2. 52 SUBPANELS ARE CLEAR.
3. 52 SUBPANELS ARE MIRRORED.
4. SUBPANEL CUTTING ARRANGEMENT AS SHOWN AT LEFT RESULTS IN MINIMUM WASTAGE.
5. SUBPANELS ARE 2 m WIDE EXCEPT AT EQUATORIAL CORNERS.

FIG. 3

CLEAR HEMISPHERE OF 32 m DIAMETER BALLOON AS SEEN FROM SUN

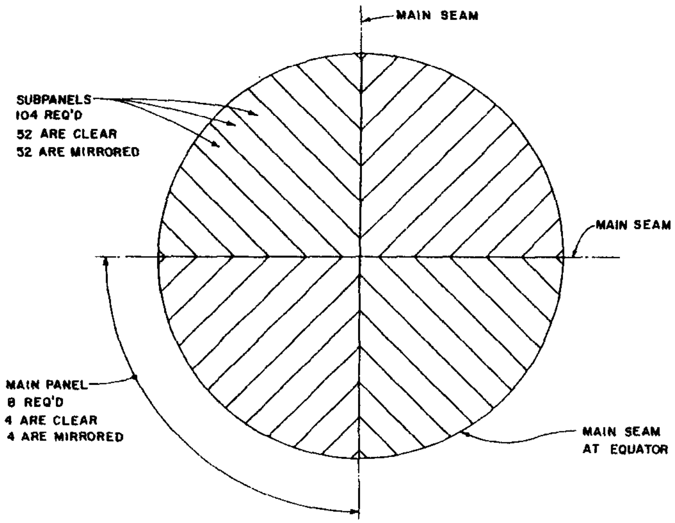

NOTES

1. VIEW IS LOOKING DOWN ON CLEAR HEMISPHERE.
2. MIRRORED HEMISPHERE IS REVERSED AND BEYOND.
3. SUBPANEL EDGE SEAMS ARE 2 m ON CENTER.
4. CLEAR HALF SEAM TAPE IS PVF FILM WITH POLYESTER MESH REINFORCEMENT AND UV RESISTANT ADHESIVE.
5. REFLECTIVE HALF SEAM TAPE IS ALUMINUM FOIL BACKED BY GLASS CLOTH WITH SODIUM SILICATE ADHESIVE.

FIG. 4

BASIC ARRANGEMENT OF A BRAZED SOLAR ENERGY COLLECTION COIL OF TUBING

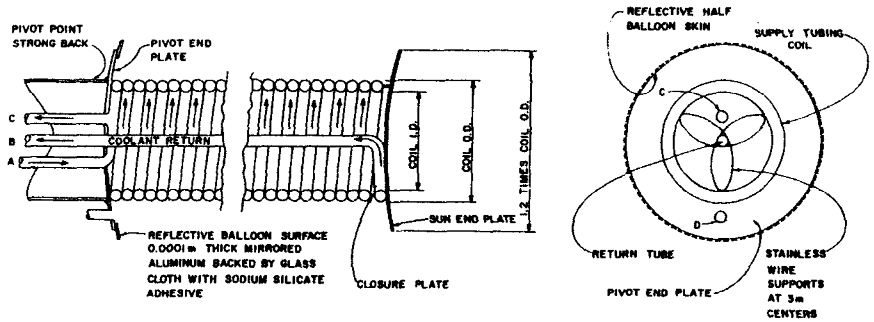

NOTES

1. A = COOLANT SUPPLY; B = COOLANT RETURN; C = VACUUM CONNECTION; AND, D = BALLOON FILL GAS CONNECTION.
2. ALL PIPING IS MINIMUM WALL THICKNESS 304L STAINLESS STEEL TUBING.
3. TUBING COIL ASSEMBLY IS ALL BRAZED OR WELDED.
4. FINISHED ASSEMBLY SHALL BE EVACUABLE TO 10^{-9} ATMA.

FIG. 5

THERMAL ELECTRIC POWER CYCLE AT 717° K MAXIMUM TEMPERATURE

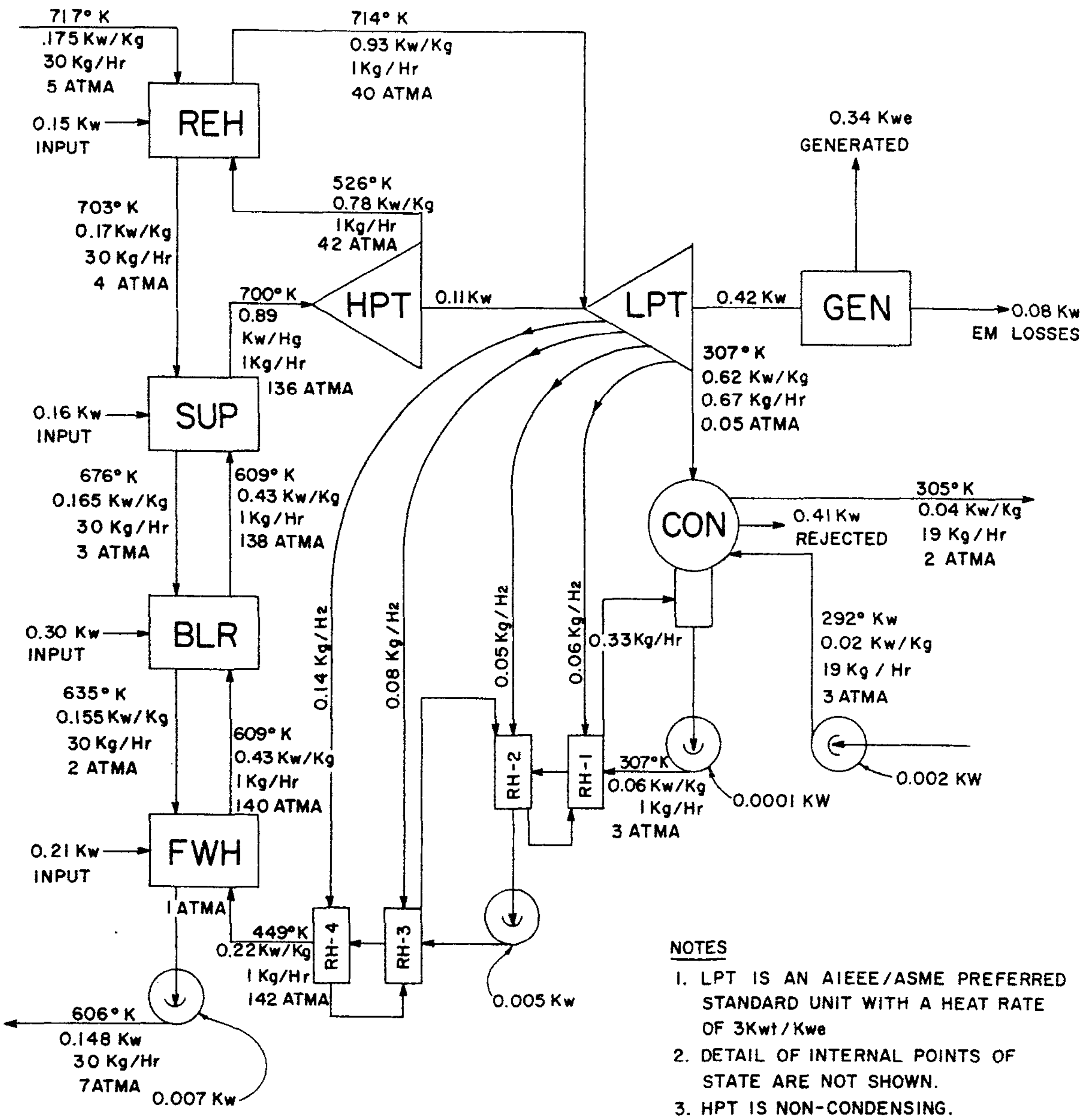

NOTES

1. LPT IS AN AIEEE/ASME PREFERRED STANDARD UNIT WITH A HEAT RATE OF 3Kwt/Kwe
2. DETAIL OF INTERNAL POINTS OF STATE ARE NOT SHOWN.
3. HPT IS NON-CONDENSING.

FIG. 6

Table 1A

C1 Balloon Diameter m Stipulated	C2 Balloon Radius Base Height m C1/2	C3 Balloon Tether Cone Diameter m C2	C4 Balloon Volume m^3 0.5236(C1**3)	C5 Balloon Half Surface m^2 1.5708(C1**2)	C6 Balloon Whole Surface m^2 2(C5)	C7 Balloon Skin Panels (Gores) Number See Note	C8 Balloon Circumference m 3.1416(C1)	C9 Great Circle Seam Length m 9.425(C1)
1	0.5	0.5	0.5	1.6	3.1	8	3.1	9
2	1	1	4.2	6.3	12.6	8	6.3	19
4	2	2	33.5	25.1	50.2	24	12.6	38
8	4	4	268.	100.5	201.	40	25.1	75
16	8	8	2,145.	402.	804.	56	50.3	151
32	16	16	17,157.	1,608.	3,217.	104	101	302
64	32	32	137,258.	6,434.	12,868.	200	201	603
128	64	64	1,098,066.	25,736.	51,472.	392	402	1,206
256	128	128	8,784,528.	102,944.	205,887.	792	804	2,413

C10 Number of Sub Seams Number See Note	C11 Length of Sub Seams m See Note	C12 Total Seam Length m C9+C11	C13 Outer Base Diam. and Slant Height m C2/0.86603	C14 Inner Base Cone Diam.& Slant Height m C13/2	C15 Outer Cone Base Area m^2 0.7854(C13**2)	C16 Outer Cone Slant Area m^2 2(C15)	C17 Outer Base Cone Surface m^2 C15+C16	C18 Inner Cone Base Area m^2 C15/4
0	0	9	0.6	0.3	0.3	0.5	0.8	0.1
0	0	19	1.2	0.6	1.0	2.1	3.1	0.3
16	32	70	2.3	1.2	4.2	8.4	12.6	1.0
32	113	188	4.6	2.3	16.8	33.5	50.3	4.2
48	432	583	9.2	4.6	67.	134.	201.	16.8
96	1,770	2,072	18.5	9.2	268.	536.	804.	67.
192	7,079	7,682	37.	18.5	1,072.	2,145.	3,217.	268.
384	28,318	29,524	74.	37.	4,289.	8,579	12,868.	1,072.
784	113,271	115,684	148.	74.	17,157.	34,315	51,472	4,289

NOTES:
C1 - These numbers are stipulated.
C2 - Each column of data is identified numerically which in this case is column "C2".
C3 - Tether off-axis angle is 60° when tether tangency diameter is one-half of balloon diameter or equal to its radius.
C4 - The factor 0.5236 is π/6 and C1**3 is C1 cubed.
C5 - The factor 1.5708 is π/2.
C6 - The second and third lines of each column heading define the subject matter as in "Balloon Whole Surface."
C7 - Each quadrant is divided by 2m width of subpanels, 2 are added for closure pieces at each side & answer is multiplied by 8.
C8 - The fourth line of each column heading identifies the dimension as in "meters."
C9 - The factor 9.425 is 3(π), as these are 3 great circle seams.
C10 - At C1 = 4 there are 3 subpanels per quadrant or 24 per balloon or 16 subseams. See Note C7.
C11 - Obtained graphically.
C13 - The factor 0.86603 is the sine of 60°.
C14 - The final line in each column heading indicates how the data was obtained which in this case is C13/2.
C15 - The factor 0.7854 is π/4.

Table 1B

C19 Inner Cone Slant Area m^2 C16/4	C20 Inner Cone Surface m^2 C18+C19	C21 Base Concrete Surface m^2 C17+C20	C22 Base Concrete Volume m^2 0.08(C21)	C23 Collector Length m C1/4	C24 Collector Diameter m C1/75	C25 Collector Projected Area m^2 3.1416(C23)(C24)	C26 Collection Area m^2 0.7854(C1**2)	C27 Concentration Factor Number C26/C25
0.1	0.2	1.0	0.1	0.25	0.013	0.01	0.8	75
0.5	0.8	3.9	0.3	0.5	0.027	0.04	3.1	75
2.1	3.1	15.7	1.3	1	0.053	0.17	12.6	75
8.4	12.6	62.8	5.0	2	0.107	0.67	50.3	75
33.5	50.3	251.	20.	4	0.213	2.68	201.	75
134.	201.	1,005.	80.	8	0.427	10.72	804.	75
536.	804.	4,021.	322.	16	0.853	42.89	3,217.	75
2,145.	3,217.	16,085.	1,287.	32	1.707	171.57	12,868.	75
8,579	12,868.	64,340.	5,147.	64	3.413	686.29	51,472.	75

C28 Balloon Skin Stress Force Kg 125(C26)	C29 Balloon Drag Kg 0.4(C28)	C30 Balloon Lift Kg 0.2(C28)	C31 Balloon Wind Force Kg 0.45(C28)	C32 Equatorial Tension Kg/m C31/C8	C33 Clear Cone Yarns/m Number 2(C32)/19	C34 Clear Cone Window Space Fraction 1-0.0005(C33)	C35 Light Reaching Collector Percent 0.838(C34)	C36 Gross Solar Energy Available Kw 0.85(C26)
98	39	19.6	44.	14	1.5	0.999	0.837	0.67
393	157	78.5	177.	28	3	0.998	0.836	2.64
1,571	628	314.	707.	56	6	0.997	0.835	10.68
6,283	2,513	1,257.	2,827.	112	12	0.994	0.833	42.73
25,133	10,053	5,027.	11,310	225	24	0.988	0.828	170.9
100,531	40,212	20,106.	45,239.	450	48	0.976	0.818	684.
402,124	160,850	80.425.	180,955.	900	95	0.952	0.798	2,734.
1,608,495	643,398	321,699.	723,821.	1,800	190	0.905	0.758	10,938.
6,433,961	2,573,593	1,286,797	2,895,282.	3,600	379	0.810	0.679	43,751.

NOTES:

C22 - The thin-wall thickness of 0.08m, about the thinnest practical for concrete construction, also provides sufficient reinforcement to resist wind forces and sufficient mass to prevent overturn at 161 Km/Hr wind velocity by a factor of 2.5.

C23 - The collector diameter is dictated by the spread angle of sun's rays incident upon the mirrored hemisphere and as reflected toward the collector and is dependent on the distance of reflection. It is close to 1.333% of balloon diameter.

C28 - Stagnant air pressure at 161 Km/Hr is 125 Kg/m^2.

C29 - Drag factor for a sphere close to and attached to ground is taken as 0.4.

C30 - Lift factor for a sphere close to and attached to ground is taken as 0.2.

C31 - Wind force is the resultant of lift and drag.

C33 - The 19 Kg design pull strength is 70% of the breaking pull of aramid yarn. Aramid yarn would have to be sheathed against UV light. Other materials such as polyester are available.

C34 - The 0.0005m diameter is based on aramid yarn, but see Note C33.

C35 - The factor of 0.838 is derived from published data. It is 0.96 transmittance through clear PVF outer surface times 0.96 through clear PVF inner surface times 0.91 reflectance from clean new aluminum.

C36 - The 0.85 factor is consensus of published data.

Table 1C

C37 Solar Energy Reaching Collector Kw (C35)(C36)	C38 Collector Heat Flux Kw/m^2 C37/C25	C39 Water Flow for Process Heating Kg/s 0.00239(C37)	C40 Water Flow for Process Heating m^3/s C39/1,000	C41 Supply and Return Header Length m 2(C2)	C42 Tube Diameter at 2m/s Velocity m (0.6366*C40)**0.5	C43 Total Supply Tube Length m C25/C42	C44 Total Tube Length m C41+C43
0.6	53.	0.001	0.0000016	1	0.001	10.3	11.3
2.2	53.	0.005	0.0000065	2	0.002	20.6	22.6
8.9	53.	0.021	0.000026	4	0.004	41.3	45.3
35.6	53.	0.085	0.000103	8	0.008	82.6	90.6
141.5	53.	0.341	0.00041	16	0.016	165.9	182.
559.	52.	1.34	0.0016	32	0.032	334.	366.
2,182.	51.	5.22	0.006	64	0.064	675.	739.
8,291.	48.	19.8	0.024	128	0.124	1,388.	1,516.
29,707.	43.	71.	0.086	256	0.234	2,933.	3,189.

C45 Water Flow Reynolds Number Number 1,770,000(C42)	C46 Water Flow Friction Factor Number From Chart	C47 Water Tube Friction Loss Atmas (C44)(C46)/203(C42)	C48 Water Pump Power in Loop Kw 0.1353(C39)(C47)	C49 Tube Thickness m at 10 atma See Note	C50 Tube Metal Volume m^3 π(C42)(C44)(C49)	C51 Tube Metal Weight Kg 7,831.4(C50)
1,800	0.057	3.1	0.00056	0.00089	0.00003	0.25
3,600	0.047	2.6	0.0019	0.00089	0.00013	0.99
7,200	0.040	2.2	0.006	0.00089	0.00055	4.33
14,400	0.034	1.9	0.022	0.00089	0.002	15.86
28,600	0.029	1.6	0.074	0.00089	0.008	63.4
56,817	0.025	1.4	0.25	0.00089	0.03	253.9
112,395	0.021	1.2	0.85	0.00089	0.13	1,013.
218,772	0.018	1.1	2.92	0.00093	0.55	4,276.
414,180	0.016	1.0	10.0	0.00176	4.1	32,218.

NOTES:

C38 - This heat flux is easily within the range of standard boiler water wall heat collection.
C39 - The 0.00239 factor is based on 100°K rise in the primary pressurized water coolant loop.
C40 - The 1,000 factor is the weight of $1m^3$ of water.
C41 - This length is based on 0.5 balloon radius for return from collector sun end plus 1.5 radii for supply and return headers external to balloon and within hollow concrete bases.
C42 - The 2m/s is a normal design velocity for water.
C43 - The spiral wind lead pitch is the pipe diameter C42.
C45 - The 1,770,000 factor is density times velocity over viscosity or 1000x2/0.00113 Kg/m-s.
C46 - The friction factor is derived from charts given in "Cameron Hydraulic Data" as taken from tentative data released by the Hydraulic Institute and required use of English units.
C47 - The 203 factor is 2gx10.363 where the 10.363 reconverts to metric units.
C48 - The 0.1353 factor is based on 90% motor efficiency and 83.33% pump efficiency for an overall efficiency of 75%.
C49 - The factor is 105,440/2x7,029,332 or 0.0075(C42). However minimum tubing thickness is 0.000889m which is used except for largest diameter tubes. The 105,440 Kg/m^2 is tube working pressure and the 7,029,332 Kg/m^2 is tube metal allowable stress.
C51 - The 7,831.4 Kg/m^3 is for steel.

Table 1D

C52 NAK Flow for TE Power Plants Kg/s 7.378(C39)	C53 NAK Flow for TE Power Plants m^3 C52/750	C54 NAK Flow Area m^2 0.7854(C42**2)	C55 NAK Flow Velocity m/s C53/C54	C56 NAK Flow Reynolds Number 70,570,000(C42)	C57 NAK Tube Friction Factor Number From Chart	C58 NAK Tube Friction Loss Atmas (C44)(C57)/203(C42)
0.01	0.000014	0.0000008	16.2	71,700	0.038	2.1
0.04	0.00005	0.0000032	16.2	143,300	0.033	1.8
0.16	0.0002	0.000013	16.2	286,500	0.030	1.6
0.6	0.0008	0.00005	16.2	572,300	0.027	1.5
2.5	0.0033	0.0002	16.2	1,140,400	0.024	1.3
9.9	0.013	0.0008	15.9	2,265,300	0.021	1.2
38.5	0.05	0.003	16.2	4,481,200	0.018	1.0
146.	0.2	0.012	16.3	8,722,500	0.016	0.9
524.	0.7	0.043	16.2	16,513,400	0.014	0.9

C59 NAK Pump Power in Loop Kw 0.1353(C52)(C58)	C60 Tether Cable Number Number 1.5708(C3)≥4	C61 Tether Cable Total Length m 0.5774(C2)(C60)	C62 Tether Cable Pull Kg 2(C31)/(C60)	C63 Tether Cable Area m^2 C62/61,500,000	C64 Tether Cable Volume m^3 (C61)(C63)	C65 Tether Cable Weight Kg 7831.4(C64)	C66 Tube Interior Volume m^3 0.7854(C42**2)(C44)
0.003	4	1.2	22.1	0.00000036	0.0000004	0.003	0.000009
0.01	4	2.3	88.4	0.0000014	0.000003	0.026	0.00007
0.035	4	4.6	353.	0.0000058	0.00003	0.21	0.0006
0.13	6	13.9	942.	0.000015	0.0002	1.66	0.005
0.45	13	60.0	1,740.	0.000028	0.0017	13.3	0.04
1.6	25	231.	3,619.	0.000059	0.014	106.4	0.3
5.4	50	924.	7,238.	0.000118	0.11	851.6	2.3
18.5	100	3,695.	14,476.	0.00024	0.87	6,801.	18.2
64.	200	14,781.	28,953.	0.00047	6.96	54,523.	137.

NOTES:

C52 - The mass flow is 7.378 times that of water because heat content is 1/4.76 and temperature range is 1.55 times larger. See Fig. 5.
C53 - The 750 factor is the weight of $1m^3$ of NAK. TE stands for thermal-electric.
C56 - The 70,570,000 factor is density times velocity over viscosity of 750x19.6/0.0002083 Kg/m-s.
C57 - See Note C46.
C60 - Each tether cable is tendrilled to cover 1m of the tether cable tangential belt so that tether cables are 2m apart at same except there should not be less than 4 tether cables.
C61 - The factor of 0.5774 is derived from 1/2x0.866 where 1 is balloon radius and 0.866 is sin 60°.
C63 - The 61,500,000 Kg/m^2 is the average of published data for stranded galvanized iron airplane cables.

Table 1E

C67 Weight of Water in Tube Kg 1,000(C66)	C68 Weight of NAK in Tube Kg 750(C66)	C69 Weight of Balloon Skin Kg 0.15(C6)	C70 Weight of Skin Reinforcement Kg 0.000435(C6)(C33)	C71 Weight of Seam Tape Kg 0.0075(C12)	C72 Weight of Deployed Skin Kg C69+C70+C71	C73 Weight of Balloon Parts Kg C65+C72	C74 Weight of Displaced Air Kg 1.1744(C4)
0.009	0.007	0.5	0.002	0.1	0.6	0.6	0.6
0.07	0.055	1.9	0.016	0.2	2.1	2.1	4.9
0.6	0.44	7.5	0.13	0.7	8.2	8.4	39.4
4.7	3.5	30.2	1.05	1.6	32.8	34.4	315.
37.3	28.	120.6	8.4	5.1	133.7	147.	2,519.
296.	222.	483.	67.2	16.3	566.	672.	20,150.
2,344.	1,758.	1,930.	537.	53.6	2,527.	3,378.	161,196.
18,191.	13,643	7,721.	4,299.	171.	12,245.	19,046.	1,289,686.
137,121.	102,841.	30,883.	34,391.	718.	66,152	120,674.	10,316.549.

C75 Weight of Balloon Gas Kg 1.1423(C4)	C76 Balloon Buoyancy Kg C74-C75	C77 Weight of Base Concrete Kg 2,482(C22)	C78 Destabilizing Forces Kg-m (C2)(C31)	C79 Stabilizing Force Kg-m (C13)(C77)/2	C80 Collector Losses at 400°K Kw 0.29(C25)	C81 Net Energy Collected at 400°K Kw 0.9(C37-C80)	C82 Collector Losses at 717°K Kw 13.873(C25)
0.6	0.02	195.	22.	56	0.003	0.54	0.06
4.8	0.1	780.	177.	450	0.012	1.97	0.23
38.3	1.1	3,119.	1,414.	3,601	0.05	7.96	0.98
306.	8.6	12,476.	11,310.	28,812	0.19	31.9	3.86
2,450.	68.8	49,903.	90,477.	230,495	0.78	126.6	15.4
19,599.	551.	199,612.	723,812.	1,843,958	3.1	500.	61.7
156,790.	4,405.	798,457.	5,790,499.	14,751,666	12.4	1,953.	247.
1,254,321.	35,365.	3,193,828.	46,323,990.	118,013,000	49.8	7,417.	988.
10,034,566.	281,983.	12,775,310.	370,591,000.	944,106,000	199.	26,557.	3,953.

NOTES:

C69 - The density of balloon skin in Kg/m^2 is based on the average of published data.
C70 - The factor of 0.000435 is derived as follows: The clear half weighs 0.00029 Kg/m^2 based on yarn density times yarn area using data previously given. The mirror half has twice as many yarns to withstand intensified stresses at the tether cable tangency circle.
C71 - The factor 0.0075 Kg/m is based on seam tape width of 0.05m.
C73 - Does not include collector tubing assembly
C74 - The factor 1.1744 is based on the density of dry air.
C75 - The factor 1.1423 is based on the density of dry nitrogen.
C76 - Above 32m diameter balloons, the balloons are weightless.
C77 - The factor 2,482 is based on the density of concrete in Kg/m^3.
C78 - This is wind force times base height.
C79 - This is concrete weight times base diameter over 2.
C80 - Heat loss factor of 0.29 Kw/m^2 is derived from formulas on pages 4-68 and 4-69 of "Mark's Standard Handbook for Mechanical Engineers," 8th Edition.
C81 - Despite the balloon skin subpanel arrangement which permits a clear see-in all the way to balloon equator the last radial 5% is suspect due to bad angle of incidence & multiple bouncing of rays reaching reflector; 10% penalty assessed at this point.
C82 - Heat loss factor of 5.76 Kw/m^2 is derived as per Note C80.

Table 1F

C83 Net Energy Collected at 717°K Kw 0.9(C37-C82)	C84 Collector Efficiency at 400°K Percent 100(C81)/C36	C85 Collector Efficiency at 717°K Percent 100(C83)/C36	C86 Maximum Temperature Difference Across Skin °K C82/0.0072(C6)	C87 Steel Area to Resist Shear m^2 C31/10,543,983	C88 Vertical Tilt Swivel Diameter m (1.273*C87)**0.5
0.49	74.6	73.1	2.7	0.000004	0.002
1.77	74.6	67.0	2.7	0.000017	0.005
7.13	74.6	66.9	2.7	0.000067	0.009
28.6	74.6	66.8	2.7	0.00027	0.018
113.5	74.1	66.4	2.7	0.00107	0.037
448.	73.1	65.5	2.7	0.0043	0.074
1,742.	71.4	63.7	2.7	0.0172	0.148
6,573.	67.8	60.1	2.7	0.069	0.296
23,179.	60.7	53.0	2.7	0.275	0.59

C89 Tracking Mount Steel Area m^2 2(C87)	C90 Tracking Mount Diameter m 1.5(C24)	C91 Tracking Mount Thickness m C89/π(C90)	C92 Tracking Mount Height m 3(C90)	93 Tracking Mount Metal Volume m^3 π(C90)(C91)(C92)	C94 Tracking Mount Weight Kg 7,831.4(C93)	C95 Weight Tubing Plus Water Kg C51+C67	C96 Collector Inside Diameter m C24-2(C42)
0.000008	0.02	0.00014	0.06	0.000000546	0.003	0.26	0.01
0.000034	0.04	0.00029	0.12	0.0000015	0.036	0.98	0.02
0.00013	0.08	0.00058	0.24	0.00003	0.24	4.92	0.04
0.00054	0.16	0.00116	0.48	0.00027	2.1	20.5	0.09
0.0022	0.32	0.00232	0.96	0.0024	17.4	100.7	0.18
0.0086	0.64	0.00358	1.92	0.015	108.3	550.	0.36
0.034	1.28	0.00927	3.84	0.15	1,122.	3,357.	0.73
0.137	2.56	0.0185	7.68	1.14	8,967.	22,467.	1.46
0.55	5.12	0.037	15.36	9.18	71,784.	169,339.	2.67

NOTES:

C83 - See Note C81.
C86 - The heat transfer factor of 0.0072 is derived from the ASHRAE Handbook.
C87 - The 10,543,983 factor is 75% of 14,058,644 Kg/m^2 which is the allowable tensile stress of steel.
C90 - The factor of 1.5 is arbitrarily selected.
C92 - The factor of 3 is arbitrarily selected.

Table 1G

C97 Collector Moment of Inertia m^4 0.0491(C24**4-C95**4)	C98 Tubing Plus Water Unit Weight Kg/m C94/C23	C99 Collector Deflection No Sun End Support m C97(C23**4)/0.1688(10^{12})(C96)	C100 Maximum Horizontal Friction Kg 0.04(C29)	C101 Horizontal Distance Per Hour m/hr π(C90)/24
0.000000008	1	0.00003	1.6	0.0026
0.000000012	2.0	0.00006	6.3	0.005
0.0000002	4.9	0.00014	25.1	0.010
0.000003	10.3	0.0003	101	0.021
0.00005	25.2	0.0008	402	0.042
0.0008	68.7	0.0021	1,609	0.084
0.0124	210	0.0066	6,434	0.17
0.194	702	0.022	25,736	0.34
4.17	2,646	0.063	102,944	0.67

C102 Maximum Rotational Power Kw (C99)(C100)/367,000	C103 Maximum Tilt Friction Kg 0.04(C30)	C104 Vertical Distance Per Hour m/hr 0.11054(C88)	C105 Maximum Tilting Power Kw (C102)(C103)/367,000	C106 Maximum Electrical Generation at 717°K at 40.5% Thermal Efficiency 0.405(C83)	C107 Balloons for a 16 Mw Plant Number 16,000/C105
0.00000001	0.8	0.0003	0.0000000005	0.198	80,808
0.00000008	3.1	0.0005	0.000000004	0.72	22,222
0.0000007	12.6	0.001	0.00000003	2.89	5,537
0.000006	50.3	0.002	0.0000003	11.6	1,380
0.00005	201	0.004	0.000002	46	348
0.0004	804	0.008	0.000018	181	89
0.0029	3,217	0.017	0.00014	706	23
0.023	12,868	0.03	0.0011	2,662	6
0.19	51,472	0.07	0.009	9,387	2

NOTES:

C97 - The 0.0491 factor is $\pi/64$.
C99 - The 0.1688(10^{12}) factor is 8 (cantilevered beam fixed at one end) times the elastic modulus of 2.11(10^{10}) Kg/m^2 for steel. Cambering can negate deflection for balloons at 128m and 256m diameter. Equatorial cabling support would be required for larger diameters.
C100 - Rolling friction is taken as 0.04 times wind drag.
C102 - The factor 367,000 is derived using standard energy units.
C103 - Rolling friction is taken as 0.04 times wind lift.
C104 - The factor of 0.11054 is πtimes 76° divided by 6 hours times 360°. The sun rises a maximum of 76° in San Francisco vicinity.
C106 - This thermal efficiency is based on the use of a 700°K, 136 atma/42 atma noncondensing high pressure turbine exhausting into a single reheater to furnish steam to a 714°K, 40 atma condensing turbine with 4 stages of regenerative heating which is an AIEEE/ASME preferred standard unit. See Fig. 5.
C107 - The 16000 Kw is derived by dividing 0.42 by 0.31, all times the 12,650 Kw rating of the AIEEE/ASME preferred standard 714°K, 40 atma condensing unit. See Fig. 5. The collector field area is constant and collector base areas are 5% of field area so that 95% of land is available for low head room use as for agriculture.

Table 1H

C108 Base Concrete Cost USD 353(C22)	C109 Collector Tubing Cost USD 13.6(C51)	C110 Tether Cable Cost USD 4.5(C65)	C111 Balloon Skin Cost USD 7(C6)	C112 Skin Reinforcement Cost USD 6(C70)	C113 Balloon Seam Tape Cost USD 6(C71)	C114 Tracking Mount Cost USD 2.67(C94)+3,000	C115 Total Unit Cost USD See Note
28	3	.01	22	0.01	0.6	3,000	3,054
111	13	.1	88	0.1	1.2	3,000	3,214
444	59	.9	352	0.8	4.0	3,001	3,861
1,774	216	7.5	1,407	6.3	9.4	3,006	6,426
7,097	862	60	5,630	50	31	3,047	16,777
28,390	3,452	479	22,519	403	98	3,289	58,631
113,560	13,772	3,834	90,076	3,224	321	5,992	230,778
454,239	58,153	30,669	360,303	25,794	1,038	26,912	956,071
1,816,956	438,170	245,352	1,441,212	206,349	4,306	194,424	4,346,768

C116 Unit Cost USD at 400°K USD/Kwt C115/C81	C117 Unit Cost Per Collection Area USD/m^2 C115/C26	C118 Unit Cost Per m of Diameter USD/m C115/C1	C119 Unit Cost Per m^2 of Balloon Surface USD/m^2 C115/C6	C120 Unit Cost USD/Kwe at 717°K USD/Kwe C115/C106	C121 End Plate Diameter m 1.2(C24)	C122 Main Panel Edge Length m See Note
5,655	3,888	3,054	972	15,424	0.02	0.79
1,631	1,023	1,607	256	4,464	0.03	1.57
485	307	965	77	1,336	0.06	3.14
201	128	803	32	554	0.13	6.28
133	83	1,049	21	365	0.26	12.57
117	73	1,832	18	324	0.5	25.13
118	72	3,606	18	327	1.0	50.27
129	74	7,469	19	359	2.0	100.53
164	84	16,980	21	463	4.1	201.06

NOTES:

C115 - Total unit cost is the summation of C107 through C113. Additional costs for lightning rod, aircraft warning lights, tether cable anchor plate and its bracing are included in the overall cost. No costs are included for engineering, site work or contingency.

C122 - Eight polar triangles, each having 90° corner angles, are required to enclose the sphere. The main panel edge length is C8/4 for all three sides.

Table II

C123 Edge Arc Pivot Radius m 1.91(C122)	C124 Equilateral Triangle Leg m 0.516(C123)	C125 Tether Ring Diameter m 2(C90)	C126 Average Strong Back Diameter m See Note
1.5	0.77	0.04	0.0225
3	1.55	0.08	0.045
6	3.10	0.16	0.09
12	6.19	0.32	0.18
24	12.39	0.64	0.36
48	24.77	1.28	0.72
96	49.55	2.56	1.44
192	99.10	5.12	2.88
384	198.20	10.24	5.76

NOTES:

C123 - Obtained graphically.
C124 - When a main panel is flat its points are the points of an equilateral triangle having legs of this length which is obtained graphically. This dimension would be used to lay out main panels followed by striking arcs and cutting the edges. This would be done on a small scale and checked before tackling larger balloons since π is an indeterminate number.
C125 - The factor of 2 is arbitrarily selected.
C126 - The average strong back diameter is selected as 0.72m for C1 = 32m and by ratio for other C1 values.